Propagation of light through an amplifying honeycomb photonic lattice

SK Firoz Islam [1], Pascal Simon [2], and Alexander A. Zyuzin [1,3]

[1] *Department of Applied Physics, Aalto University, P.O. Box 15100, FI-00076 Aalto, Finland*

[2] *Université Paris-Saclay, CNRS, Laboratoire de Physique des Solides, F-91405 Orsay, France*

[3] *Ioffe Physical–Technical Institute, St. Petersburg 194021, Russia*

(Received 30 May 2020; accepted 18 September 2020; published 7 October 2020)

We consider light propagation through a ballistic amplifying photonic honeycomb lattice below the lasing threshold. Two sublattices of the system are formed by waveguides with different complex dielectric permittivities, which results in the non-Hermitian Dirac equation for electromagnetic fields. We reveal that there exists a critical length of the amplifying region for which the photonic lattice exhibits an amplifier-to-generator transition. The transmission and reflection probabilities at the normal angle of incidence are strongly enhanced at a critical length of the system. We also comment on the sensitivity of amplification to the direction of incident light and the thickness of the amplifying region.

DOI: 10.1103/PhysRevA.102.043504

I. INTRODUCTION

A two-dimensional (2D) photonic lattice (PhL) [1,2] has emerged as a versatile platform in engineering the optical analogs of most of the interesting quantum phenomena related to the nontrivial band topology occurring in 2D condensed matter systems [3–6]. In particular, it was first noted that a periodic array of parallel waveguides, forming a triangular lattice, can split the dispersion curves by an absolute gap in frequency [1]. Tamm surface waves were shown to exist at frequencies within the band gap for certain lattice terminations [7]. It was later shown that photonic crystals might have Dirac points in the band structure at certain frequencies [1,2]. Analogs of the quantum Hall effect and of the anomalous quantum effect have been proposed by utilizing the interplay of broken spatial inversion and time-reversal symmetries and the band-structure topology at the Dirac point [2,8]. Reviews on the optical analogs of the electronic band structure and transport properties can be found in Refs. [5,9–12].

Let us specify that the scattering phenomena in a Dirac material such as graphene differ fundamentally from the electronic system described by a quadratic band structure [13,14]. In a certain regime of parameters, the Dirac electron can fully tunnel through the potential barrier without any reflection, a phenomenon known as Klein tunneling. A photonic analog of Klein tunneling was also investigated in PhL and a transition from unit transmission to full reflection of the electromagnetic (EM) wave with respect to the band-structure deformation was found [15]. The effects of the interfacial coupling between air media and a PhL on the EM wave transmission through a PhL was also investigated [16]. The possibility of a negative refractive index has recently been predicted by studying EM wave transmission though the driven-dissipative background [17].

However, detailed studies of the Klein tunneling process of an EM wave through a 2D honeycomb PhL with an amplifying background are lacking. The effect of such a background on the EM wave transmission through photonic crystals has already attracted intense research interests after the theoretical proposals of a parity-time ($\mathcal{PT}$) symmetric laser absorber [18] and a laser as a coherent perfect absorber [19]. This has further been boosted by a series of works which are reviewed, for example, in Ref. [11]. Very recently, several artificial techniques of imparting non-Hermiticity in the 2D honeycomb PhL have been reported, which opened up the possibility of an experimental realization of Klein tunneling through a loss or gain medium [5,11,12].

Here, we take this advantage to investigate the EM wave propagation through an amplifying PhL at the vicinity of a Dirac point in the spectrum of a wave. The amplification background is attributed to the imaginary part of the dielectric constants of the waveguides. We find that there exists a critical length of the amplifying region for which the transmission and reflection probabilities diverge, i.e., resonance does occur. Above the threshold, there exists a generator solution. For the limiting case of the scattering problem for an imaginary delta-function potential, the resonance condition is related to a critical strength of the barrier. We also comment on the effect of an imaginary gauge field on the transmission probability, which is known to exponentially suppress transmission in preferred directions of light propagation [20,21].

II. NON-HERMITIAN HAMILTONIAN

We consider a 2D PhL in an x-y plane formed out of cylindrical waveguides aligned parallel to the z axis. These waveguides are arranged in a way to form a hexagonal cross section, mimicking the graphene geometry by replacing each sublattice point with a waveguide. The 2D cross section of the PhL is described by a frequency-dependent dielectric constant $\varepsilon_\omega(x, y)$ which is periodic in the x-y plane. We consider a simple setup which consists of two regions with positive and real dielectric permittivities (regions I and III) separated by an

amplifying region II of length L_x. The interior of the waveguides in region II has a complex dielectric permittivity, which describes the response of oscillating dipoles of frequency ω_0.

Here, in order to derive the wave equation for the propagation of an EM field in a photonic honeycomb lattice, we follow Refs. [1,22] for explicit derivations. Let us start with the Helmholtz equation for the z component of the EM field $\sim E_z(x, y)e^{-i\omega t}$, passing through the PhL, as

$$\left[\varepsilon_\omega^{-1}(x, y)\nabla^2 + \omega^2/c^2\right]E_z(x, y) = 0, \tag{1}$$

where c is the speed of light. In regions I and III, the periodic arrangement of waveguides allows us to employ the Bloch theorem. The field component E_z on the honeycomb lattice can be written using irreducible singlet and doublet representations for two sets of inequivalent corners of the hexagonal first Brillouin zone. The doublet states form a Dirac point, while nondegenerate singlet states are well separated in frequency from the Dirac points and will be ignored. One can show that the field satisfies the Dirac-like eigenvalue equation (see Ref. [5] for a review)

$$(\Omega + iv\boldsymbol{\sigma}\cdot\boldsymbol{\partial})E = 0, \tag{2}$$

where $\Omega = (\omega^2 - \omega_D^2)/\omega_D$ in which ω_D is the frequency of the band touching point, v is the velocity term, and $\sigma_{x,y,z}$ are the Pauli matrices. Note that the above Dirac-like band structure appears for both modes [6]: the transverse electric (TE) mode ($E_z = 0, H \neq 0$) and the transverse magnetic (TM mode) ($E_z \neq 0, H_z = 0$), but at different frequencies (ω_D) with a different velocity parameter (v).

The optical medium with a loss and gain background might be described by a non-Hermitian Dirac Hamiltonian, whose unique feature is the emergence of exceptional points or lines, where the complex frequency eigenvalues coalesce [11,23–25]. In region II, the complex dielectric constant inside the waveguides results in complex additive terms in the wave equation as (for details of the derivation, see, for example, Ref. [22])

$$(\tilde{\Omega} + iv\boldsymbol{\sigma}\cdot\boldsymbol{\partial} + i\Gamma + i\gamma\sigma_z + i\epsilon\sigma_x)E = 0, \tag{3}$$

where $\tilde{\Omega} = (\omega^2 - \tilde{\omega}_D^2)/\tilde{\omega}_D$ denotes the frequency of the band touching point in region II, $\tilde{\omega}_D \neq \omega_D$. The negative (positive) values of Γ determine the overall gain (loss) in the system, while γ describes the difference in the amplification (dissipation) between the two sublattices. Note that while the imaginary term $i\gamma\sigma_z$ violates both spatial inversion symmetry as well as time-reversal symmetry, the $i\Gamma$ breaks only the latter. The last term, $i\epsilon\sigma_x$, is the imaginary gauge field which might stem from an imaginary magnetic flux [20]. In what follows, we consider an amplifying system $\Gamma < 0$ with $|\Gamma| > |\gamma|, |\epsilon|$ and shall comment further on the other cases.

III. SCATTERING THROUGH AMPLIFYING MEDIA

Let us now discuss how the amplifying background affects the ballistic transmission of an EM wave through a PhL. We consider the standard scattering problem by seeking for transmission and reflection probabilities of the incident radiation in the geometry, as shown in Fig. 1. We shall assume that the wave vector parallel to the interfaces is conserved as well the radiation frequency at the Dirac point, namely $\omega = \tilde{\omega}_D$.

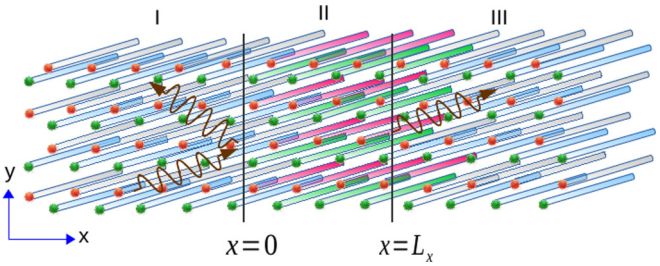

FIG. 1. Schematic sketch of the device. Two different colors are used to denote the A and B sublattice (here, waveguides). The waveguides in region II, of length L_x, are embedded into a non-Hermitian background for which different colors are used. Regions I and III are considered to be identical and quite longer than region II. In region II, the waveguides are filled with media described by a complex dielectric permittivity.

The problem is analogous to the scattering problem through a rectangular potential barrier in graphene [13,14], except that the real potential barrier is replaced by a complex one.

The eigenstates in regions I and III corresponding to Eq. (2) can be written, respectively, as

$$\begin{aligned} E_1(x, y) &= [n\chi_+ e^{ik_x x} + r\chi_- e^{-ik_x x}]e^{ik_y y}, \\ E_3(x, y) &= t\chi_+ e^{i(k_x x + k_y y)}, \end{aligned} \tag{4}$$

where the spinor part is given by $\chi_\pm = [1, v(\pm k_x + ik_y)/\Omega]^T$. The reflection and transmission amplitudes are denoted by r and t. The wave vector can be parametrized with the angle of incidence as $vk_x = |\Omega|\cos\theta$ and $vk_y = |\Omega|\sin\theta$.

Inside the amplifying region II, the propagation of light is dominated by the evanescence mode at $\omega = \tilde{\omega}_D$. The eigenstate corresponding to Eq. (3) can be written as

$$E_2(x, y) = [a\psi_+ e^{-\kappa x} + b\psi_- e^{\kappa x}]e^{ik_y y}e^{-\epsilon x/v}, \tag{5}$$

where the spinor part of the solution is given by $\psi_\pm = [1, v(\pm\kappa + k_y)/(\Gamma - \gamma)]^T$ and κ can be determined from $v\kappa = \sqrt{v^2k_y^2 + \Gamma^2 - \gamma^2}$. The effect of γ on backscattering at the normal angle of incidence can be seen from the spinor structure of the solution.

Note that unlike the case of a Hermitian scattering problem, here the energy of the incident flux is not conserved. It is rather amplified or absorbed which can be expressed by the continuity equation as [26,27]

$$\frac{\partial j}{\partial x} + \frac{\partial N}{\partial t} = 2E_2^\dagger(\Gamma + \gamma\sigma_z + \epsilon\sigma_x)E_2. \tag{6}$$

Here, j and N denote the energy flux density and the wave intensity density of the EM wave, respectively. The right-hand side of the above equation defines the increase or decrease of incident flux density while passing through region II. The degree of amplification can be quantified by a coefficient [26,27] as

$$\alpha(\theta) = \frac{j_t - j_r}{j_i} - 1 = \frac{2}{v\cos\theta}\int_0^{L_x} E_2^\dagger(\Gamma + \gamma\sigma_z + \epsilon\sigma_x)E_2 dx, \tag{7}$$

where j_i, j_r, and j_t are the incident, reflected, and transmitted flux densities, respectively.

Using the continuity condition for the wave function across the interfaces at $x = 0$ and $x = L_x$, one has

$$n\chi_+ + r\chi_- = a\psi_+ + b\psi_-,$$
$$a\psi_+ e^{-\kappa L_x} + b\psi_- e^{\kappa L_x} = t\chi_+ e^{ik_x L_x} e^{\epsilon L_x/v}. \quad (8)$$

The above two equations can be solved to obtain the transmission probability $T = tt^*/n^2$ as

$$T(\theta) = \frac{[v\kappa \cos\theta/\sinh(\kappa L_x)]^2 e^{-2\epsilon L_x/v}}{[\Gamma + v\kappa\cos\theta\coth(\kappa L_x)]^2 + \Omega^2\sin^4\theta}. \quad (9)$$

The reflection probability $R = rr^*/n^2$ is given by

$$R(\theta) = \frac{\Gamma^2\sin^2\theta + (\gamma\cos\theta + \Omega\sin\theta)^2}{[\Gamma + v\kappa\cos\theta\coth(\kappa L_x)]^2 + \Omega^2\sin^4\theta}. \quad (10)$$

Taking the difference of energy flux between the left and right regions, one notes $\alpha(\theta) = T(\theta) + R(\theta) - 1$.

Let us discuss the behavior of the transmission and reflection probabilities. At $\gamma = 0$ and normal incidence of light, the reflection probability is zero, while the transmission through amplifying media increases compared to unity, respectively, as $T(0) = e^{2(|\Gamma|-\epsilon)L_x/v}$. The backscattering effect of γ can be seen in the appearance of the resonance in transmission probability at the normal angle of incidence. This is in contrast to the electron Klein tunneling problem in graphene [13,14]. Indeed, in the amplifying media at $\Gamma < 0$, one obtains

$$\tanh\left(\frac{L_x|\Gamma|}{v}\sqrt{1-\gamma^2/\Gamma^2}\right) = \sqrt{1-\gamma^2/\Gamma^2}. \quad (11)$$

The solution of the above equation describes the situation of the generator threshold, at which region II acts as a source of the radiation in the absence of the incident field, i.e., at $n = 0$. At $|\Gamma| \gg |\gamma|$ the threshold length of the system logarithmically diverges with the decrease of $|\gamma|$ as $L_{x,\mathrm{cr}} \approx (v/|\Gamma|)\ln|2\Gamma/\gamma|$, while at $\sqrt{\Gamma^2-\gamma^2}L_x/v \ll 1$ one has $L_{x,\mathrm{cr}} \approx v/|\Gamma|$ and the transmission probability at the normal angle of incidence is enhanced as

$$T(0) = \frac{e^{-2\epsilon/|\Gamma|}}{(1-|\Gamma|L_x/v)^2}. \quad (12)$$

The reflection probability at the normal angle of incidence is strongly increased at the vicinity of threshold $R(0) = (\Gamma/\gamma)^2/(1-|\Gamma|L_x/v)^2$, which is opposite to the reflectionless Klein tunneling through graphene lattice in the Hermitian case. The system becomes a generator if $L_x > L_{x,\mathrm{cr}}$, so that there are finite solutions for $R(0)$ and $T(0)$ at vanishing incident radiation.

We plot the transmission and reflection probabilities in Fig. 2 under an amplification background at the vicinity of the critical length. Both $T(\theta)$ and $R(\theta)$ are enhanced at the critical length as show in Figs. 2(a) and 2(b), respectively. Moreover, notice that $R(\theta)$ is not symmetric with respect to the angle of incidence due to the term $i\gamma\sigma_z$ in Eq. (3), which indicates that the reflected wave picks up an additional phase from the small imbalance in loss and gain between two waveguides. This asymmetry in reflection probability is a direct manifestation of inversion symmetry breaking. The asymmetry decreases with reducing the length L_x and the frequency Ω, which can be seen from Eq. (10). Changing the sign of γ leads to a mirror symmetric plot of the angle dependence of reflection

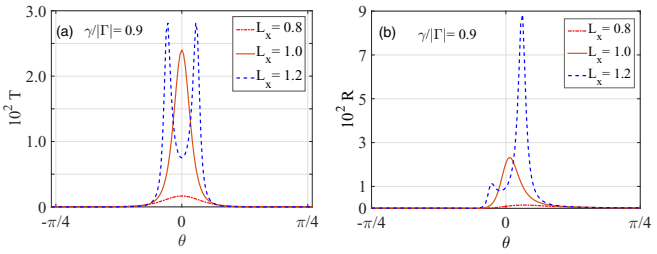

FIG. 2. (a) Transmission and (b) reflection probabilities as a function of the angle of incidence θ under an amplification background. The different lengths are taken in units of $L_{\mathrm{cr}} = v/|\Gamma|$ and $\Omega/|\Gamma| = 5$ and $\epsilon = 0$. The case with negative γ is described by the mirror symmetric plots.

probability. So far we study the case $\tilde{\Omega} = 0$. We note that the deviation of $\tilde{\Omega}$ from the zero value inside the amplifying region suppresses the amplitude of the resonance as shown in the plots of $T(\tilde{\Omega}, \theta)$ and $R(\tilde{\Omega}, \theta)$ in Fig. 3.

Finally, the amplitude of the transmission probability is sensitive to the direction of the incident wave due to the complex term ϵ [20,21]. Note that expressions in Eq. (9) are obtained for the wave incident from the left side. To find the transmission probability of the wave incident from the right, one has to substitute $e^{-2\epsilon L_x/v} \to e^{+2\epsilon L_x/v}$ in Eq. (9). At $|\epsilon|L_x/v > 1$, one of the two scattering processes shall be exponentially suppressed, although the resonance condition Eq. (11) is independent on ϵ.

The peak in $T(\theta)$ and $R(\theta)$ gets split into two with a further increase of length beyond the critical value. This case cannot be described by the solution of the linear equation and the saturation has to be taken into account. The dielectric constant depends on the photon flux density $i\Gamma \to i\Gamma(1 - E^\dagger\eta E)$, where the components of the matrix η describe saturation of the stimulated emission [5,11]. Let one keep γ and ϵ fixed and tune the pump $|\Gamma|$ over the threshold value $|\Gamma_{\mathrm{cr}}|$ defined by Eq. (11). Above the threshold, the field in the middle region is given by $E_2 = a\psi$, with

$$\psi = \left\{\psi_+ e^{-\kappa x} + \frac{|\Gamma|}{\gamma}[\sqrt{1-\gamma^2/\Gamma^2} - 1]\psi_- e^{\kappa x}\right\} e^{ik_y y - \epsilon x/v}, \quad (13)$$

where the weak nonlinearity $0 < E^\dagger\eta E < |\gamma/\Gamma|$ determines the amplitude of the solution,

$$|a|^2 = (1 - |\Gamma_{\mathrm{cr}}/\Gamma|)\frac{\int_0^{L_x} dx|\psi|^2}{\int_0^{L_x} dx|\psi|^2(\psi^\dagger\eta\psi)}, \quad (14)$$

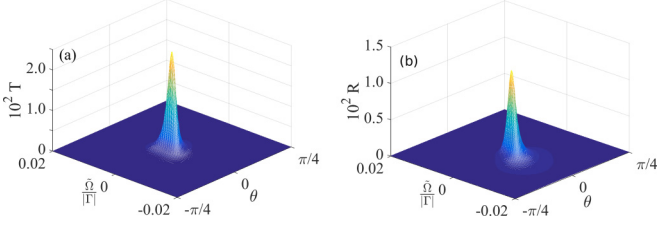

FIG. 3. (a) Transmission and (b) reflection probabilities are shown in the plane of $(\tilde{\Omega}/|\Gamma| - \theta)$ at the length $L_{\mathrm{cr}} = v/|\Gamma|$. All other parameters are the same as in Fig. 2.

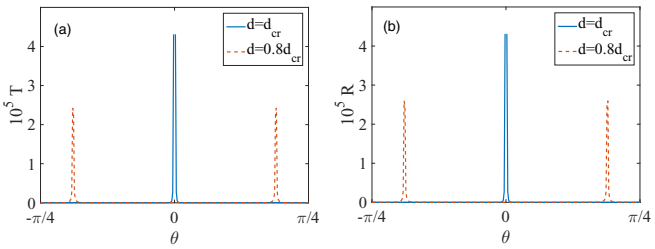

FIG. 4. Resonance in (a) transmission and (b) reflection probabilities. Here, $d_{\rm cr} \sim v/|\Gamma|$ and all other parameters are same as in Fig. 2.

where $|\Gamma/\Gamma_{\rm cr}|$ are the coefficients of the excess of the pump over the threshold value.

IV. THIN SCATTERING REGION

Let us also comment on the case when the amplifying region is very thin $L_x \to d$ and strong so that $|\Gamma|, |\gamma| \gg |\tilde{\Omega}|$, where $d = v/\Lambda$ is the short-range cutoff with the frequency width Λ, within which the model of a Dirac-like spectrum is valid. This can be realized by plugging all the waveguides along the y direction at $x = 0$. Here, the transmission probability is given by

$$T(\theta) = \left[\frac{v\kappa\cos\theta/\sinh(d\kappa)}{\Gamma + v\kappa\cos\theta\coth(d\kappa)}\right]^2 e^{-2\epsilon d/v}, \tag{15}$$

and the reflection probability (for $\epsilon = 0$) can be obtained as

$$R(\theta) = \frac{\Gamma^2\sin^2\theta + \gamma^2\cos^2\theta}{[\Gamma + v\kappa\cos\theta\coth(d\kappa)]^2}. \tag{16}$$

The resonance survives in the thin limit $L_x \to d$, provided the condition $d|\Gamma|/v \sim 1$ is satisfied. However, apart from the normal incidence, the resonance can also be seen for any arbitrary angle, provided $v\kappa\cos\theta_c = \Gamma\tanh(d\kappa)$ for the amplifying background. The amplitude of the solution inside the thin region can also be obtained by incorporating the above-mentioned limits. We plot the transmission and reflection probabilities in Fig. 4, which shows that the resonance can occur at a normal angle of incidence as well as away from the normal incidence for different parameters. It is also interesting to note that the width and height of the resonance peak are much sharper in contrast to the wide junction case [see Fig. 2], which is attributed to the extra term $\Omega^2\sin^4\theta$ in the denominator of Eq. (9). It can also be clearly seen that the effects of the imaginary gauge field (ϵ) remain insensitive to the thickness of the junction. The reflection probability is fully suppressed at normal incidence without inversion symmetry breaking, $\gamma = 0$.

V. DISCUSSION

We shall also comment on the propagation of the radiation through the photonic honeycomb lattice with dissipation at $\Gamma > |\gamma|, |\epsilon|$. Suppose that the incident light is coming on the dissipative media from both regions I and III. The resonance condition at which the amplitude of the reflecting waves vanishes can be understood from the fact that the divergence of $T(0)$ in Eq. (9) depends on the sign of $\Gamma\cos\theta$. Note that the spinor of the wave incident on the media from the right side acquires a sign reversal of $\cos\theta \to \cos(\pi - \theta)$. Hence the pole in the amplitude of the incoming waves takes place at positive Γ. In this case the system acts as an absorber of the radiation above the threshold Eq. (11) with an absorption coefficient $-1 < \alpha < 0$.

The interplay of non-Hermiticity and topology in 2D PhL has been extensively considered in the last decade [5,12] including the $\mathcal{PT}$-symmetric case with balanced loss and gain (see, for example, Refs. [22,28]). However, resonances in the ballistic transmission of light through a honeycomb PhL with such a background have been overlooked so far. We consider a honeycomb PhL under a uniform amplification or dissipation to each waveguide, i.e., a broken $\mathcal{PT}$-symmetric lattice. The PhL can provide emission or perfect absorption of light above a certain threshold length. Here, the resonant feedback is due to an inversion symmetry breaking term in the Dirac-like wave equation. We should also mention that the imaginary gauge field has no impact on the generator threshold in our model, although it leads to an exponential enhancement or suppression of the transmission probability, which is sensitive to the direction of incident light. The effect of the imaginary gauge field remains robust to the thickness of the amplifying junction.

It is also instructive to consider the effect of multiple light scatterings at a pointlike defect, which is described by a potential $i\gamma\sigma_z\delta(\mathbf{r} - \mathbf{r}_i)$ at a position $\mathbf{r} = \mathbf{r}_i$. The Green's function of Eq. (3) at $\epsilon = 0$ and under the substitution $i\gamma\sigma_z \to i\gamma\sigma_z\delta(\mathbf{r} - \mathbf{r}_i)$ in the presence of the single impurity satisfies an equation

$$[\tilde{\Omega} + i\Gamma + i\gamma\sigma_z\delta(\mathbf{r} - \mathbf{r}_i) + iv\boldsymbol{\sigma}\boldsymbol{\partial}_r]\mathcal{G}(\mathbf{r}, \mathbf{r}') = \delta(\mathbf{r} - \mathbf{r}'), \tag{17}$$

where the Green's function is normalized to ω_D^2/c. To obtain the possible localized or trapped states, we solve the impurity scattering problem by computing the poles of the T matrix, which can be found from the equation $\det[1 + i\gamma\sigma_z\mathcal{G}(\mathbf{r}_i, \mathbf{r}_i)] = 0$, where the bare Green's function is given by

$$\mathcal{G}(\mathbf{r}_i, \mathbf{r}_i) = -\frac{\tilde{\Omega} + i\Gamma}{4\pi v^2}\ln\frac{\Lambda^2}{(\Gamma - i\tilde{\Omega})^2}. \tag{18}$$

One obtains two equations for the poles,

$$(\Gamma - i\tilde{\Omega})\ln\frac{\Lambda^2}{(\Gamma - i\tilde{\Omega})^2} = \pm\frac{4\pi v^2}{\gamma}. \tag{19}$$

At the Dirac point, in the limit of a large potential $|\gamma| \gg v^2/\Lambda$, the poles for both amplifying and dissipative media are given by $\Gamma = \pm 2\pi v^2/\gamma\ln|\gamma\Lambda/2\pi v^2|$.

Finally, besides the resonant feedback, it has been long known that disorder might provide a feedback for generation of light [29]. The properties of the random laser have been extensively studied (for a review, see Ref. [30]). It would be interesting to extend the above results to the light propagation through disordered amplifying photonic honeycomb lattices.

VI. CONCLUSION

To conclude, we investigate the propagation of the electromagnetic wave through an amplifying region in a photonic

honeycomb lattice. We reveal that there exists a critical length of the amplifying region for which the transmission and reflection probabilities of the wave diverge at a normal angle of incidence. The condition for the generator threshold is determined by the parameters associated with the lattice structure and amplification background. The amplification is sensitive to the direction of the incident wave in the presence of an imaginary gauge field in the amplifying region. We also comment on the resonant states in a thin scattering region. The possible existence of localized states in the presence of a single impurity is also discussed. Our investigation on resonance might be realized in realistic setups, designed in honeycomb photonic or plasmonic lattices [28,31], where such feedback has been artificially imparted.

ACKNOWLEDGMENTS

This work is supported by the Academy of Finland Grant No. 308339. A.A.Z. is grateful for the hospitality of the Pirinem School of Theoretical Physics.

[1] M. Plihal and A. A. Maradudin, Photonic band structure of two-dimensional systems: The triangular lattice, Phys. Rev. B **44**, 8565 (1991).

[2] F. D. M. Haldane and S. Raghu, Possible Realization of Directional Optical Waveguides in Photonic Crystals with Broken Time-Reversal Symmetry, Phys. Rev. Lett. **100**, 013904 (2008).

[3] F. D. M. Haldane, Model for a Quantum Hall Effect without Landau Levels: Condensed-Matter Realization of the Parity Anomaly, Phys. Rev. Lett. **61**, 2015 (1988).

[4] G. Volovik, in *The Universe in a Helium Droplet*, edited by W. van Haeringen and D. Lenstra (Oxford University Press, Oxford, U.K., 2003).

[5] T. Ozawa, H. M. Price, A. Amo, N. Goldman, M. Hafezi, L. Lu, M. C. Rechtsman, D. Schuster, J. Simon, O. Zilberberg, and I. Carusotto, Topological photonics, Rev. Mod. Phys. **91**, 015006 (2019).

[6] B. A. Khanikaev, S. H. Mousavi, W.-K. Tse, M. Kargarian, A. H. MacDonald, and G. Shvets, Photonic topological insulators, Nat. Mater. **12**, 233 (2012).

[7] W. M. Robertson, G. Arjavalingam, R. D. Meade, K. D. Brommer, A. M. Rappe, and J. D. Joannopoulos, Observation of surface photons on periodic dielectric arrays, Opt. Lett. **18**, 528 (1993).

[8] M. Onoda, S. Murakami, and N. Nagaosa, Hall Effect of Light, Phys. Rev. Lett. **93**, 083901 (2004).

[9] H. van Houten and C. W. J. Beenakker, in *Analogies in Optics and Micro Electronics*, edited by W. van Haeringen and D. Lenstra (Kluwer, Dordrecht, 2007).

[10] L. Lu, J. D. Joannopoulos, and M. Soljačić, Topological photonics, Nat. Photonics **8**, 821 (2014).

[11] V. V. Konotop, J. Yang, and D. A. Zezyulin, Nonlinear waves in $\mathscr{PT}$-symmetric systems, Rev. Mod. Phys. **88**, 035002 (2016).

[12] V. M. Alvarez Martinez, J. E. Barrios Vargas, M. Berdakin, and L. E. F. Foa Torres, Topological states of non-Hermitian systems, Eur. Phys. J. Spec. Top. **227**, 1295 (2018).

[13] M. I. Katsnelson, K. S. Novoselov, and A. K. Geim, Chiral tunnelling and the Klein paradox in graphene, Nat. Phys. **2**, 620 (2006).

[14] P. E. Allain and J. N. Fuchs, Klein tunneling in graphene: Optics with massless electrons, Eur. Phys. J. B **83**, 301 (2011).

[15] O. Bahat-Treidel, O. Peleg, M. Grobman, N. Shapira, M. Segev, and T. Pereg-Barnea, Klein Tunneling in Deformed Honeycomb Lattices, Phys. Rev. Lett. **104**, 063901 (2010).

[16] R. A. Sepkhanov, Ya. B. Bazaliy, and C. W. J. Beenakker, Extremal transmission at the Dirac point of a photonic band structure, Phys. Rev. A **75**, 063813 (2007).

[17] T. Ozawa, A. Amo, J. Bloch, and I. Carusotto, Klein tunneling in driven-dissipative photonic graphene, Phys. Rev. A **96**, 013813 (2017).

[18] S. Longhi, $\mathscr{PT}$-symmetric laser absorber, Phys. Rev. A **82**, 031801(R) (2010).

[19] Y. D. Chong, L. Ge, H. Cao, and A. D. Stone, Coherent Perfect Absorbers: Time-Reversed Lasers, Phys. Rev. Lett. **105**, 053901 (2010).

[20] S. Longhi, D. Gatti, and G. Valle, Robust light transport in non-Hermitian photonic lattices., Sci. Rep. **5**, 13376 (2015).

[21] S. Longhi, D. Gatti, and G. Della Valle, Non-Hermitian transparency and one-way transport in low-dimensional lattices by an imaginary gauge field, Phys. Rev. B **92**, 094204 (2015).

[22] X. Ni, D. Smirnova, A. Poddubny, D. Leykam, Y. Chong, and A. B. Khanikaev, $\mathscr{PT}$ phase transitions of edge states at $\mathscr{PT}$ symmetric interfaces in non-Hermitian topological insulators, Phys. Rev. B **98**, 165129 (2018), (see the Supplemental Material).

[23] C. M. Bender and S. Boettcher, Real Spectra in Non-Hermitian Hamiltonians Having $\mathscr{PT}$ Symmetry, Phys. Rev. Lett. **80**, 5243 (1998).

[24] M. Berry, Physics of nonhermitian degeneracies, Czech. J. Phys. **54**, 1039 (2004).

[25] K. Kawabata, K. Shiozaki, M. Ueda, and M. Sato, Symmetry and Topology in Non-Hermitian Physics, Phys. Rev. X **9**, 041015 (2019).

[26] Z. Ahmed, Schrödinger transmission through one-dimensional complex potentials, Phys. Rev. A **64**, 042716 (2001).

[27] P. Molinàs-Mata and P. Molinàs-Mata, Electron absorption by complex potentials: One-dimensional case, Phys. Rev. A **54**, 2060 (1996).

[28] M. Kremer, T. Biesenthal, L. J. Maczewsky, M. Heinrich, R. Thomale, and A. Szameit, Demonstration of a two-dimensional $\mathscr{PT}$-symmetric crystal, Nat. Commun. **10**, 435 (2019).

[29] V. S. Letokhov, Generation of light by a scattering medium with negative resonance absorption, Zh. Eksp. Teor. Fiz. **53**, 1442 (1968) [Sov. Phys. JETP **26**, 835 (1968)].

[30] D. S. Wiersma, The physics and applications of random lasers, Nat. Phys. **4**, 359 (2008).

[31] R. Guo, M. Nečada, T. K. Hakala, A. I. Väkeväinen, and P. Törmä, Lasing at k Points of a Honeycomb Plasmonic Lattice, Phys. Rev. Lett. **122**, 013901 (2019).